Personal Account

DOI: 10.1002/tcr.201500257

THE CHEMICAL RECORD

N-Modified Carbon-Based Materials: Nanoscience for Catalysis

Laura Prati,*[a] Carine E. Chan-Thaw[a], Sebastiano Campisi[a], and Alberto Villa[a]

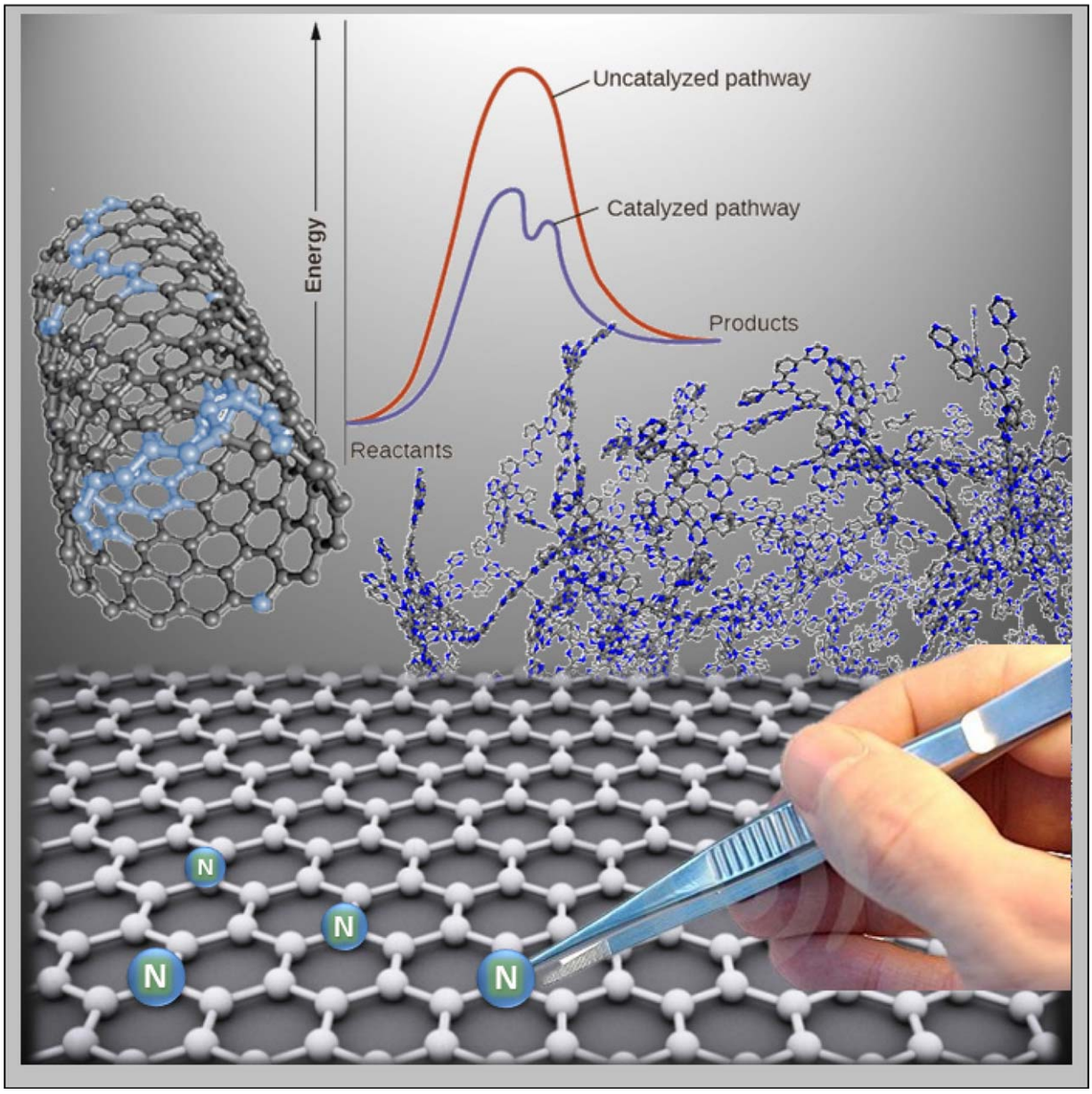

ABSTRACT: Carbon-based materials constitute a large family of materials characterized by some peculiarities such as resistance to both acidic and basic environments, flexibility of structure, and surface chemical groups. Moreover, they can be deeply modified by simple organic reactions (acid–base or redox) to acquire different properties. In particular, the introduction of N-containing groups, achieved by post-treatments or during preparation of the material, enhances the basic properties. Moreover, it has been revealed that the position and chemical nature of the N-containing groups is important in determining the interaction with metal nanoparticles, and thus, their reactivity. The modified activity was addressed to a different metal dispersion. Moreover, experiments on catalysts, showing the same metal dispersion, demonstrated that the best results were obtained when N was embedded into the carbon structure and not very close to the metal active site.

Keywords: carbon, doping, covalent organic frameworks, nanotubes, supported catalysts

1. Introduction

Carbon-based materials can be roughly divided into crystalline and amorphous. Both materials present high resistance to acidic/basic environments, which makes these materials suitable for use under a wide range of conditions. They can undergo relatively easy functionalization, which represents an attractive way to tune the surface properties.

One of the most studied covalent derivatizations is based on the chemistry of oxygenated functionalities (Figure 1), the number of which can be increased by oxidative treatment in strongly acidic media and where carboxylic groups dominates.

Functionalities are normally present on edges/corners of crystalline domains or on sidewall defects of graphene sheets. It is not surprising therefore that the number of functionalities decrease in the order active carbons (ACs)>graphite, carbon nanotubes (CNTs), graphene>diamonds. Figure 2 presents, as an example, different Raman and X-ray photoelectron spectroscopy (XPS; O 1s region) results that highlight the differences between O-containing functionalities of graphite and AC (X40S Camel).[1]

Moreover, in the case of synthetic materials, the introduction of functionalities can be realized not only as post-synthesis treatment, but also using selected reagents. P or S constitutes an example for the doping of mesoporous ordered carbons (OMCs) prepared by a soft templating technique in the presence of H_2SO_4 or H_3PO_4 mineral acids.[2]

A different approach that provides a higher flexibility in terms of functional groups is the case of a covalent organic framework (COF) based on a C backbone formed through controlled polymerization of organic moieties. In this case, different functional groups of the monomer can be used to link the units and to provide additional functional groups (Figure 3).

In the last few years, particular attention was paid to the introduction of basic groups within the carbon structure, and particularly N-containing groups to modify the acid/base properties of carbon materials. Our group, in particular, was interested in studying the impact of N-functionalities on the catalytic properties of metal-catalyzed oxidation reactions, in which a basic environment speeds up the reaction and influences the selectivity. The aim of the whole study has been to clarify the role of the nature, amount, and position of the N-functional groups on the catalytic performance.

2. Covalent Triazine Frameworks (CTFs)

Kuhn and co-workers developed a new class of COFs produced from the trimerization of aromatic nitriles in molten $ZnCl_2$; so-called covalent triazine frameworks (CTFs).[3] This dynamic reorganization of porous polymers with the selected carbonitrile groups, namely, *para*−1,4-dicyanobenzene (DCB) and 2,6-dicyanopyridine (DCP) lead to the formation of covalent triazine frameworks (CTF_{DCB} and CTF_{DCP} respectively; Figure 4). Because of the variety of aromatic nitriles, the significant surface area and amounts of nitrogen functionalities can be tuned in the network. Thanks to their covalent structures, the CTFs were found to be stable thermally and chemically. Therefore, CTFs are excellent candidates as supports in liquid-phase reactions.

Likewise, the electronic structures in CTF_{DCB} are ruled by both the number of stacking layers and the ratio of different aromatic rings, as suggested by Sakaushi and co-workers.[4] Moreover, CTFs is an ambipolar organic material that can act as an organic semiconductor. The benzene rings are electron

[a]L. Prati, C. E. Chan-Thaw, S. Campisi, A. Villa
Department of Chemistry
Università degli Studi di Milano
via C.Golgi 19
20133 Milano
(Italy)
E-mail: Laura.Prati@unimi.it

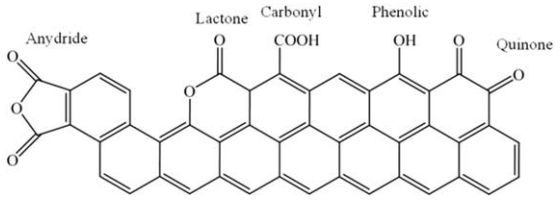

Fig. 1. Oxygenated groups in C-based structures.

donors and the triazine rings are electron acceptors. Additionally, CTFs can also be used as both a cathode and an anode; therefore, CTFs can be used as an energy storage material[5] and as photocatalysts.[6] Herein, we describe the utilization of CTFs as a new generation of heterogeneous catalysts. Palkovits and co-workers were the first to study CTFs as catalytic supports.[7] Indeed, they coordinated Pt along a pyridine-bridged covalent triazine framework (Pt-CTF) to produce a heterogeneous Periana catalyst. This Pt-CTF catalyst showed a high stability in methane oxidation under harsh conditions, namely, concentrated sulfuric acid at 215°C. Indeed, after several reaction cycles, no degradation of the support was observed. Moreover, the introduction of functionalities has been investigated on other carbon supports and resulted in an enhanced catalytic performance.[8]

Our group utilized CTFs as supports for palladium nanoparticles (NPs) for the liquid-phase oxidation of glycerol, for which stabilization of the metal NPs on the support is one of the major challenges.[9] The Pd-supported catalysts were prepared by the sol immobilization technique ($NaBH_4$/polyvinyl alcohol (PVA)) to ensure better dispersion of the small (about 3 nm) Pd NPs on the support (Figure 5).[10] When compared with Pd-supported activated carbon, the Pd-supported CTFs were more resistant to deactivation and more selective toward glycerate. The noteworthy stability of Pd/CTF in three runs is directly associated with diminished Pd leaching, and limited Pd NPs growth observed by TEM during the course of the reaction. These conclusions are explained by better interactions between the Pd NPs and nitrogen functionalities present in the structure, and therefore, leading to a homogeneous distribution of metal NPs.

He et al. also highlighted the positive effect of adding Pd to CTF for the catalytic hydrogenation of N-heterocycles compared with the traditional Pd/AC.[11] They also attributed the better catalytic activity to good dispersion and narrow distribution of the Pd NPs on the CTFs, thanks to the anchoring effect of the N functionalities.

Having established the positive effect of the nitrogen heteroatoms on the catalytic oxidation of glycerol, we further continued our investigation by modulating the nitrogen content of the support.[12] We immobilized Pd NPs on g-C_3N_4, CTF_{DCB}, and CTF_{DCP} to test these catalysts in the oxidation of benzyl alcohol (alcohol/metal: 5000, $T = 80°C$, $pO_2 = 2$

Laura Prati has been Associate Professor of Inorganic Chemistry at the Università degli Studi di Milano since 2001. She received her specialization in "Tecniche Analitiche per la Chimica Organica Fine" from the Politecnico di Milano in 1985 and was awarded a Ph.D. in Industrial Chemistry in 1988. For several years she has been applying low-impact environmental catalytic methodologies as alternative processes to stoichiometric ones in organic synthesis. Her scientific interests focus principally on the specific design of heterogeneous catalysts.

Carine E. Chan-Thaw is an Assistant Researcher at the University of Milan. Her Ph.D. research was carried out at the Fritz Haber Institute under the supervision of Prof. Robert Schlögl. She received a European PhD in Chemistry, 2008, from both the Université de Strasbourg and the Technische Universität Berlin. She accepted a postdoctoral fellowship at the Technische Universität Berlin, where she worked on testing nitrogen-rich, highly porous frameworks for liquid-phase oxidations. She is currently investigating the valorization of biomass.

Sebastiano Campisi is a Ph.D. student at the Department of Chemistry of the Università degli Studi di Milano. His research interests include the design of nanostructured catalysts for the valorization of biomass-derived compounds and the use of *Operando* spectroscopy for the characterization of catalytic solid–liquid interfaces. Recently, he has been involved in the DFT modelling of heterogeneous catalysts for alcohol oxidation.

Alberto Villa is an Assistant Professor at the University of Milan. He received his Ph.D. in Industrial Chemistry in 2007 from the University of Milan, where his thesis focused on the development of gold-based catalysts for liquid-phase reactions. After postdoctoral research at the Fritz Haber Institute of Berlin (2008–2009), he accepted a position at the University of Milan. His current research focuses on the development of noble-metal-free heterogeneous catalysts for biomass transformation. He has (co)authored over 70 publications in peer-reviewed journals.

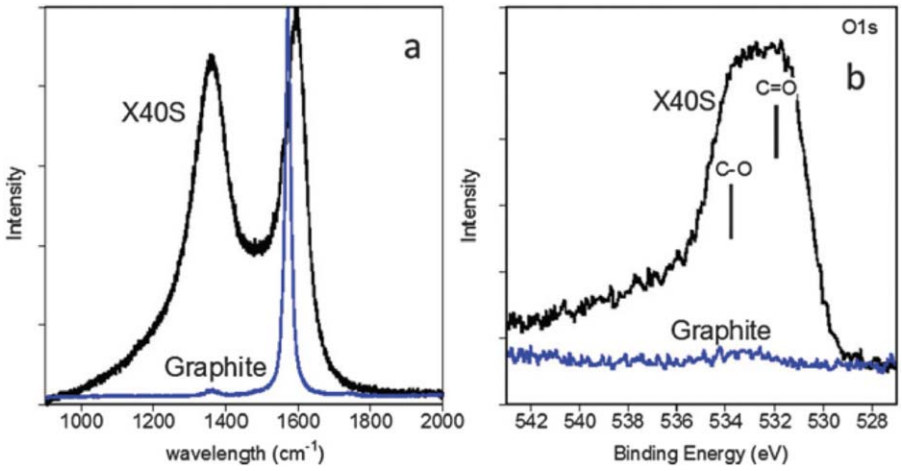

Fig. 2. Raman and XPS results for graphite (blue) and AC X40S (black). Reproduced from ref. [1] with permission from the PCCP Owner Societies.

atm, benzyl alcohol/cyclohexane ratio 50/50), and compared their activity. Pd/C, a nitrogen-free palladium catalyst and the reference catalyst for our target reaction, had a lower activity (2678 mol Pd^{-1} h^{-1}) than our three catalysts (14131, 8025, and 4917 mol Pd^{-1} h^{-1} for Pd/C_3N_4, Pd/CTF_{DCP}, and Pd/CTF_{DCB}, respectively).[12b]

Despite similar Pd NP sizes (3.18, 3.16, and 3.09 nm for Pd/CTF_{DCB}, Pd/C_3N_4, and Pd/CTF_{DCB} respectively) and Pd oxidation states, substantial differences in catalytic activity were observed. Moreover, the small difference in the generated pH of CTF_{DCP} (5.45) and C_3N_4 (6), highlighting the low basicity of both supports, cannot be responsible for the enhanced activity of Pd/C_3N_4 compared with that of Pd/CTF_{DCP}

We therefore used XPS and elemental analysis results to emphasize a direct correlation between the enhancement of the activity and an increase in the nitrogen content of the catalyst (Figure 6).

Indeed, changes in the nitrogen functionality of the Pd-supported catalysts and the original support material were examined by XPS. For both CTF_{DCP} and C_3N_4 support materials, there is a decrease in C_2NH functionality with the addition of Pd that can only be correlated to the interaction of Pd with these sites (Figure 7).

Moreover, in the case of CTF_{DCP} and C_3N_4, two distinct trends of the N content was revealed by the C/N/O distribution. After deposition of the Pd NPs, an increase in the amount of N (from 14 to 30%) was observed in the case of CTF_{DCP}, whereas a decrease in N was detected for C_3N_4 (57 to 28%). This observation is the direct consequence of the preferential deposition of Pd NPs on the N adsorption sites of C_3N_4, leading to strong electronic modification of Pd NPs. Therefore, an intimate correlation between the increase in activity and amount of N groups during the benzyl alcohol oxidation was established.

Another benefit of using CTFs as support materials in liquid-phase reaction lies in their outstanding ability to stabilize the formation of 2.6 nm PdH_x particles within the pores.[13] To establish such aptitude, a concise study on the possible effect of the preparation technique has been carried out. In addition to the sol immobilization technique previously used, the impregnation method (IMP) was also applied. IMP would theoretically lead to the confinement of Pd within the pores of CTF (Pd_{IMP}/CTF), which would result in enhanced stability of Pd/CTF. Such confinement would imply monitoring of the properties of the materials and tunability of their reactivity.

To underline our assumption, a Pd XPS study was performed and it revealed a lower Pd intensity (XPS signal = 0.2 at % Pd) for Pd_{IMP}/CTF than that observed for Pd_{PVA}/CTF (3.0 at % Pd), despite identical 1% Pd weight loading. Moreover, an overview TEM image gives a 2.6 nm Pd NP size, which perfectly matches the mean pore size of CTF determined by nitrogen adsorption (2.7 nm), as reported elsewhere.[3b] Furthermore, TEM images also emphasize a high metal dispersion and narrower distribution of Pd particle sizes

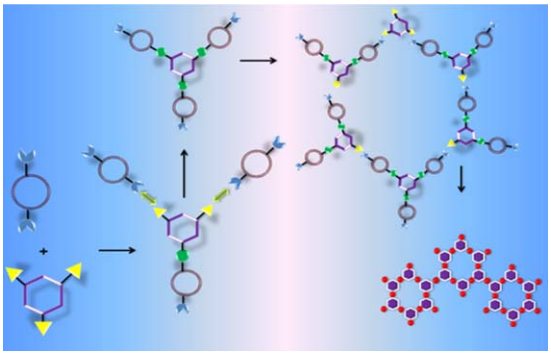

Fig. 3. Illustration of COF formation.

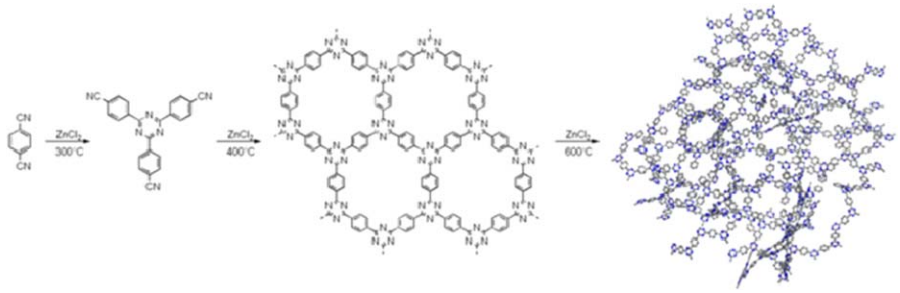

Fig. 4. Reaction scheme for the formation of the CTF. Reprinted with permission from ref. [9]. Copyright 2010 American Chemical Society.

without the presence of large particles. Combining both characterization methods, it could be suggested that most of the Pd particles are embedded within the CTF structure and not at the external surface, which was the case with the Pd_{PVA}/CTF catalyst. We therefore investigated the Pd oxidation states and, astonishingly, although reduced with $NaBH_4$ only oxidized Pd ($Pd^{\delta+}$) was found in Pd_{IMP}/CTF, as in the case of non-reduced $Pd(II)_{IMP}$/CTF. When reduced with H_2, again only $Pd^{\delta+}_{IMP}$/CTF was obtained, and we concluded that, if no reduced Pd was detected, the CTF network should stabilize oxidized PdH_x species. This statement was later confirmed by high-resolution (HR) TEM analyses on more than 100 Pd particles for the Pd_{IMP}/CTF catalyst. A purely metallic Pd unit cell parameter is 3.89 Å, whereas that measured in Pd_{IMP}/CTF, in which the Pd particles were in a face-centered cubic arrangement, averaged (4.01 ± 0.057) Å (Figure 8). Moreover, the (111) and (200) lattice spacing values on more than 100 Pd particles did not fit with any of Pd oxide phases, but matched perfectly to the lattice of PdH_x, signifying that H could only be introduced into the Pd lattice during reduction with $NaBH_4$.[14] The formation of PdH_x (x>0–0.7) species has already been already reported in the literature: the authors reduced Pd NPs embedded in a Zr-modified mesoporous SiO_2 by $NaBH_4$.[15] Hydrogen, which was introduced during the reduction treatment, was desorbed during an in situ heating treatment at 400°C of the catalyst on a Gatan heating holder in a transmission electron microscope, as already reported elsewhere.[16]

These three catalysts, Pd_{PVA}/CTF, Pd_{IMP}/CTF, and $Pd(II)_{IMP}$/CTF were tested in the glycerol oxidation reaction, and the obtained activity and selectivity further indicated the presence of PdH_x species.

The unreduced catalyst was 35% active after 4 h, implying possible in situ reduction of the Pd oxide inside the CTF network. Moreover, when performing an XPS study on the used Pd_{IMP}/CTF catalyst, 60% Pd^0 was detected, which suggested the reduction of the Pd ions during contact with glycerol and derivatives.

A key point of this study derives from the difference in selectivity between Pd_{PVA}/CTF and Pd_{IMP}/CTF (Table 1). In the case of Pd_{PVA}/CTF, the formation of C_3 products (glyceric and tartronic acids) are favored, as expected from previous study, with a selectivity of 81% at 90% conversion to glyceric

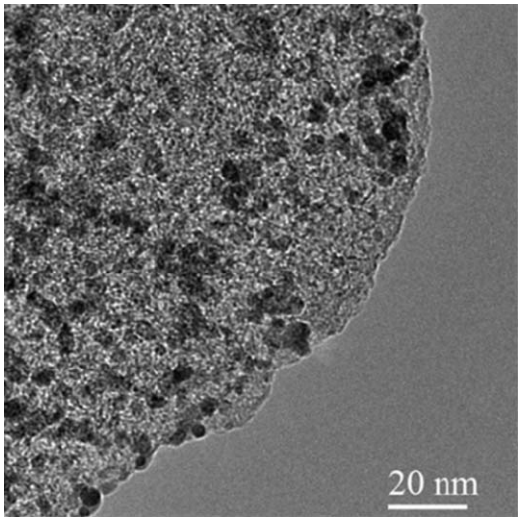

Fig. 5. TEM image of 1 wt % Pd/CTF catalyst before reaction. Reprinted with permission from ref. [9]. Copyright 2010 American Chemical Society.

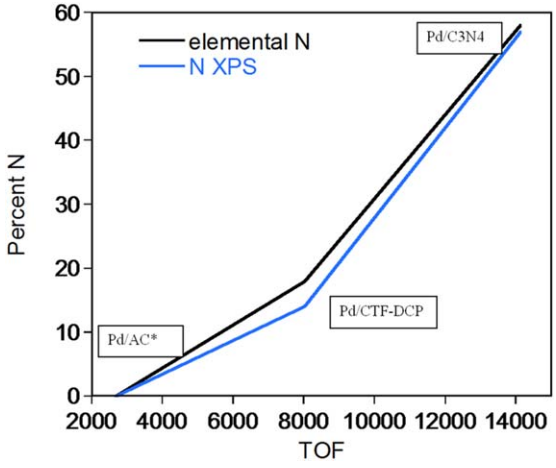

Fig. 6. Activity of the catalyst as a function of the nitrogen concentration Reproduced by permission from ref. [12b]. Copyright © 2013 Wiley-VCH.

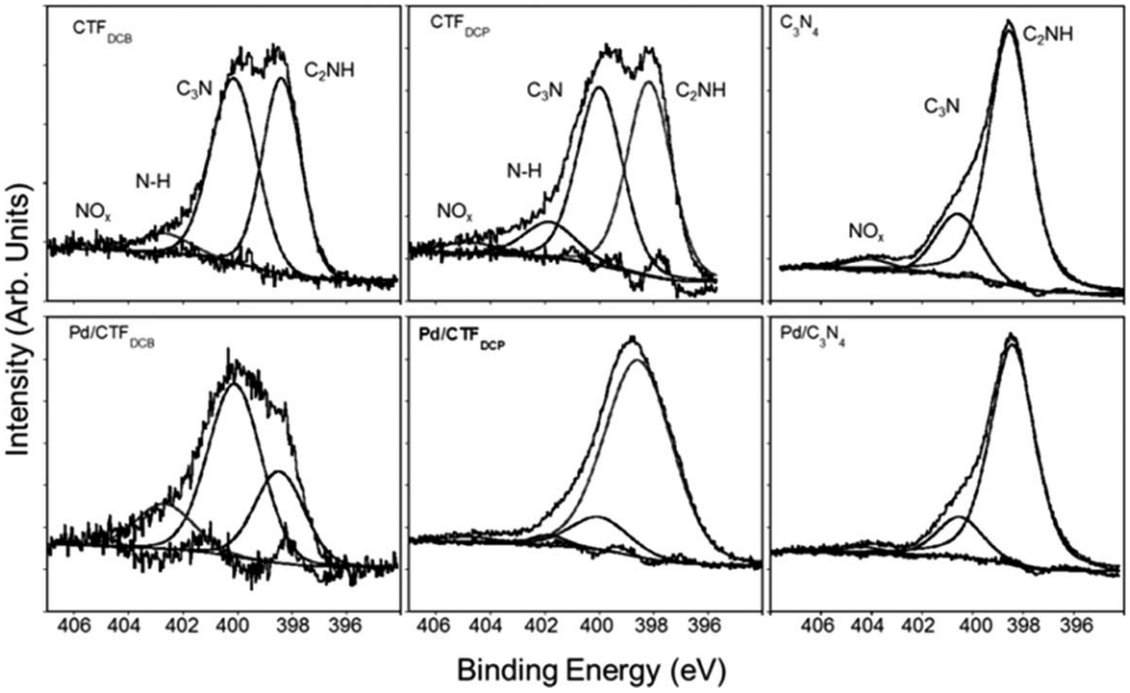

Fig. 7. XPS measurements on the three supports and catalysts Pd/CTF_{DCB}, Pd/C_3N_4, and Pd/CTF_{DCP}. N 1s XPS data. Reproduced with permission from ref. [12b]. Copyright © 2013 Wiley-VCH.

acid. On the other hand, at the same conversion, a lower amount of glyceric acid (62%) and a non-negligible amount of C_2 products (12 and 6% for respectively glycolic and oxalic acids, respectively) were obtained with Pd_{IMP}/CTF. This distinguished selectivity would suggest the undeniable contribution of hydride particles present in Pd_{IMP}/CTF. It is therefore proposed that PdH_x species would directly reduce O_2 to generate H_2O_2, which favors C–C cleavage, leading to a higher formation of C_2 products (Scheme 1).[17]

To highlight the difference between the two preparations of catalysts (Pd_{PVA}/CTF and Pd_{IMP}/CTF), their respective durability over nine runs (4 h each) was studied (Figure 9). The Pd_{PVA}/CTF catalyst deactivates consistently from the fourth run, whereas Pd_{IMP}/CTF exhibits almost the same conversion over the nine runs. The slight decrease of activity could be explained by a slight loss of catalyst during filtration from one cycle to the next and physicochemical stabilization due to confinement of the Pd NPs inside the framework. However, the selectivity to glyceric acid increased persistently (Table 2). This evolution in glyceric acid selectivity suggests a constant decrease in PdH_x species during recycling, as confirmed by XPS.

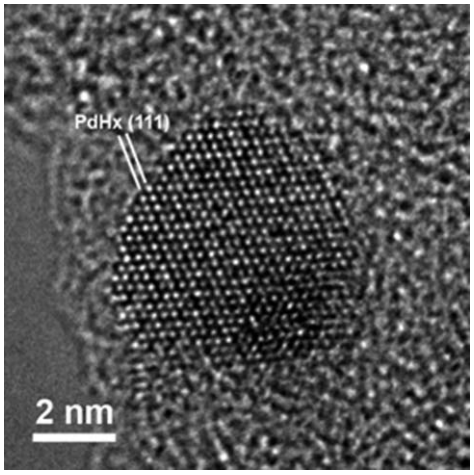

Fig. 8. HRTEM image of Pd_{IMP}/CTF with enlarged (111) lattice spacing, corresponding to a lattice parameter of 4.01 Å. Reproduced with permission from ref. [13]. Copyright © 2015 Wiley-VCH.

Table 1. Selectivity of Pd_{PVA}/CTF and Pd_{IMP}/CTF for glycerol oxidation.[a]

	Selectivity at 90% conversion			
Catalyst	Glyceric acid	Glycolic acid	Oxalic acid	Tartronic acid
Pd_{PVA}/CTF	81	4	3	12
Pd_{IMP}/CTF	62	12	6	18

[a]Reaction conditions: 0.3 M NaOH/glycerol ratio = 4 mol/mol, glycerol/metal: 1000 mol/mol, 3 atm O_2 and 50°C. Adapted with permission from ref. [13]. Copyright © 2015 Wiley-VCH.

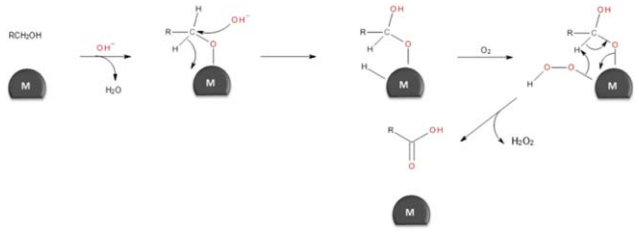

Scheme 1. Accepted mechanism of metal-catalyzed glycerol oxidation. Reproduced with permission from ref. [13]. Copyright © 2015 Wiley-VCH.

3. N-Doped CNTs (N-CNTs)

CNTs can be ideally considered as rolled graphene sheets; therefore, constituting a sp^2-carbon surface without any additional groups, except conjugated double bonds. Indeed, functionalities can be found on the tube ends or defects on the wall surface.[18] To introduce additional groups, we have to break the ordered carbon structure, which is normally achieved by an oxidative treatment (HNO_3; Figure 10). This is the main reason why O-containing functionalities are the most well studied starting points for subsequent transformation.[19]

The introduction of N functionalities can be performed by high-temperature treatment in the presence of NH_3.[20] The overall structure of the CNT is not appreciably affected by this treatment (Figure 11).

The nature of the N groups and their relative amounts depends on the thermal treatment. Titration of basic sites showed an increased number of moles of basic sites per gram by increasing the temperature (4.5×10^{-4} at 473K, 6×10^{-4} at 673K, and 10×10^{-4} at 873K).[21] Moreover, six different species of N-containing groups were detected (Figure 12). XPS investigations revealed that pyridine-like moieties are favored at low temperature (473K), whereas nitro or N-oxide are favored at higher temperature (873K; Figure 13).[22]

It appears that all N groups contribute to increased metal dispersion when preformed metal NPs are deposited on the doped CNTs. As shown in Table 3, a single metallic sol (Au), showing a mean size of 2.45 nm with a standard deviation (σ) of 0.27, behaves differently during the immobilization step, depending on the presence or absence of N functionalities.

The enhancement in metal dispersion observed in the presence of N groups is also confirmed by TEM investigations

Table 2. Selectivity to glyceric acid during the recycling of Pd_{IMP}/CTF (4 h of reaction).[a]

Runs	1	2	3	4	5	6	7	8	9
$S_{glyceric\ acid}$ [%]	62	56	64	58	70	73	84	79	80

[a]Reaction conditions: 0.3 M, NaOH/glycerol ratio = 4 mol/mol, glycerol/metal: 1000 mol/mol, 3 atm O_2 and 50°C. Adapted with permission from ref. [13]. Copyright © 2015 Wiley-VCH.

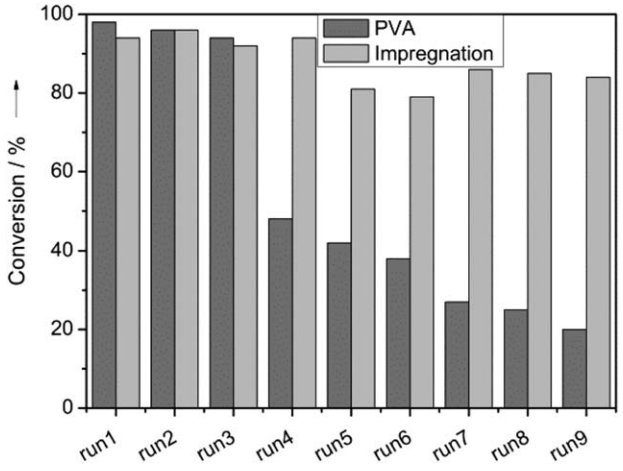

Fig. 9. Conversion during recycling (4 h) of 1 wt % Pd_{PVA}/CTF and 1 wt % Pd_{IMP}/CTF. Reproduced with permission from ref. [13]. Copyright © 2015 Wiley-VCH.

(Figure 14). It should be noted that the parent support only treated with HNO_3 showed values closer to that of pristine CNTs than to those of N-CNTs (statistical median 3.65 nm with a standard deviation of 0.78). This is a clear indication that the N groups are more effective than O groups at improved metallic dispersion. This trend also proved to be effective in the case of Pd preformed NPs, as reported in Table 4.

In principle, this finding would positively affect any metal-catalyzed reaction, but especially in alcohol oxidation, for which the basic environment is important and the basicity of the support is also beneficial.

Indeed, upon testing these N-doped catalysts for alcohol oxidation, we observed enhanced activity with respect to the pristine support.[23] Table 5 reports the results obtained for benzyl and cinnamyl alcohol oxidation to the corresponding aldehyde.

The results clearly indicated the superior activity of Pd supported on N-doped CNTs, but the weight of the two different contributions (of metal dispersion and basicity) could be debated. Therefore, in a subsequent study, the catalysts were tested in a different reaction under strongly basic conditions;

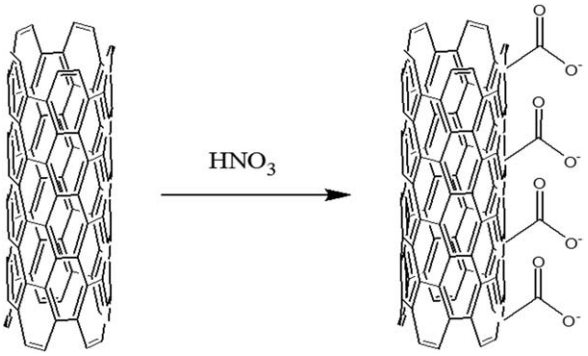

Fig. 10. Oxidative treatment of CNTs by HNO_3.

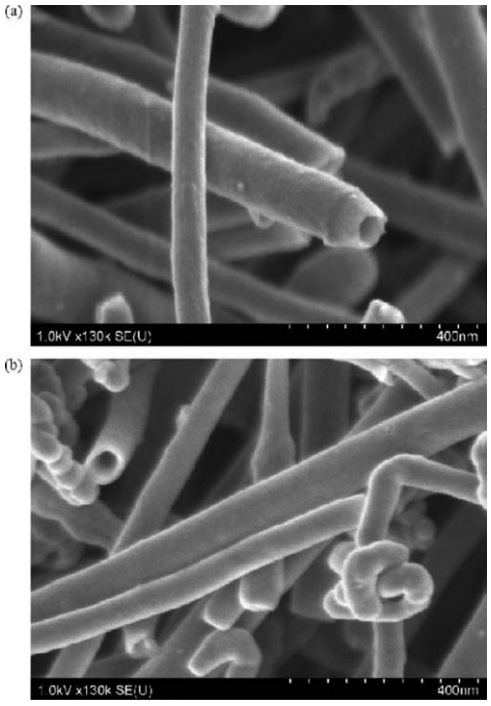

Fig. 11. SEM overview of CNTs a) before and b) after NH_3 treatment. Reprinted with permission from ref. [5].

thus removing the contribution of the basicity of the support. The glycerol oxidation reaction catalyzed by Au was chosen.[21] Even in this case, we observed an extraordinary effect on the activity passing from Au on pristine CNT to N-doped CNTs (Table 6). Moreover, Au on oxidized CNT showed an almost similar activity than Au/CNT in agreement with the very similar size and distribution of Au particles. In this case, it was then possible to conclude that the activity of the catalysts was ruled out by the dimension of the metal NPs.

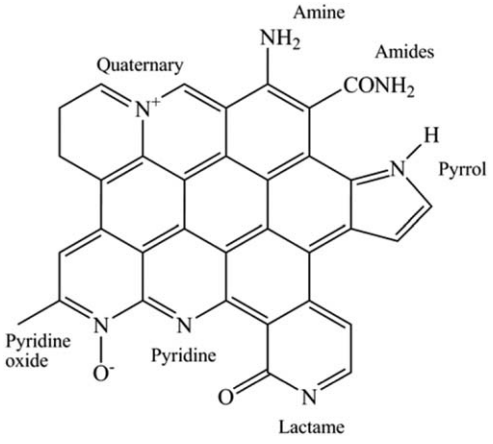

Fig. 12. Different nitrogen groups introduced in CNTs by thermal treatment with NH_3.

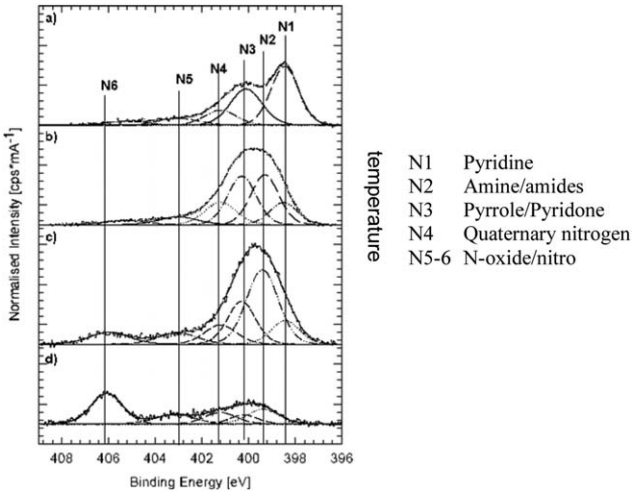

Fig. 13. XPS N 1s signal evolution with *T* during thermal treatment with NH_3: a) 473 K; b) 673K; c) 873K; d) oxidized CNTs without thermal treatment with NH_3. Reprinted with permission from ref. [22]. Copyright (2008) American Chemical Society.

However, looking at the product distribution (measured at iso-conversion), it is possible to observe that pristine and oxidized CNTs present a higher tendency to cleave C–C bonds; thus producing a higher amount of glycolate than N-CNTs (Table 6). Many studies, however, stated that, in glycerol oxidation, selectivity depended on metal particle dimensions: larger particles were more selective to glyceric acid than smaller ones. Based on this trend, we would expect the

Table 3. Au NP size on CNT and N-CNT.[a]

	Au sol	Au/CNT	Au/N-CNT 473 K	Au/N-CNT 873 K
Statistical median [nm]	2.45	3.80	3.15	2.94
Standard deviation (σ)	0.27	0.95	0.57	0.51

[a]From HRTEM measurements (data from ref. [21]).

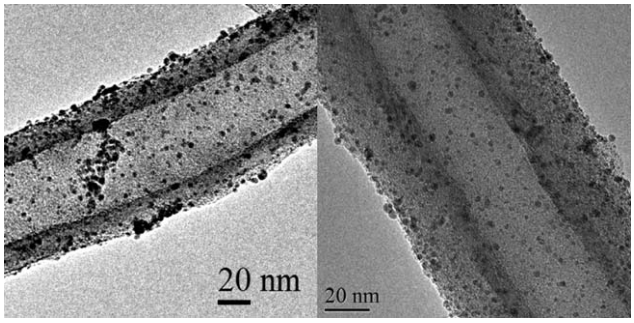

Fig. 14. TEM images of a) Au/CNT and b) Au/N-CNT at 873 K. Reproduced from ref. [1g] with permission from The Royal Society of Chemistry.

Table 4. Statistical median and standard deviation of particle size analysis for Pd-based catalysts.[a]

	Pd sol	Pd/CNT	Pd/N-CNT 873 K
Statistical median [nm]	2.80	4.28	3.28
Standard deviation (σ)	0.27	1.41	0.93

[a]From HRTEM measurements (data from ref. [21]).

opposite behavior for Au/CNT and Au/N-CNT. A possible explanation is related to different kinetics of decomposition of H_2O_2 generated during the reaction (see Scheme 1). Indeed, a lower decomposition of H_2O_2 would allow the peroxide to react with glycerol to produce a higher amount of glycolate. However, in this case, H_2O_2 decomposition is dominated by the strongly basic conditions, and thus, we would expect the contribution of H_2O_2 in regulating the product distribution to be very similar in both cases.

Therefore, additional relevant factors from a catalytic point of view should be present.

A recent study was carried out with the aim of further investigating the role of N doping. To avoid any problems correlated with different particle sizes due to the presence or absence of N groups, an AC was used as the support.[24] In fact, AC, differently from pristine CNT, assures a high metal dispersion.

Table 5. Effect of support N-doping for benzyl/cinnamyl alcohol oxidation with Pd/CNT catalysts.[a]

	Benzyl alcohol		Cinnamyl alcohol	
Pd/CNT	TOF [h^{-1}]	Selectivity[a]	TOF [h^{-1}]	Selectivity[a]
Pristine	10	92	52	75
N-doped	836	93	494	76

[a]Reaction conditions: 0.3 M in water, alcohol/metal: 1/500 mol/mol, 1,5 atm O_2 and 60°C (data from ref. [23]).

Table 6. Effect of support N-doping in glycerol oxidation with Au/CNT catalysts.[a]

		Selectivity at 90% conversion		
Au/CNT	TOF [h^{-1}]	Glycerate	Glycolate	Tartronate
Pristine	182	55	27	<1
Oxidized	186	65	20	<1
N-doped (873K)	853	68	13	14

[a]Reaction conditions: 0.3 M, NaOH/glycerol ratio = 4 mol/mol, glycerol/metal: 1000 mol/mol, 3 atm O_2 and 50°C. Data from ref. [21].

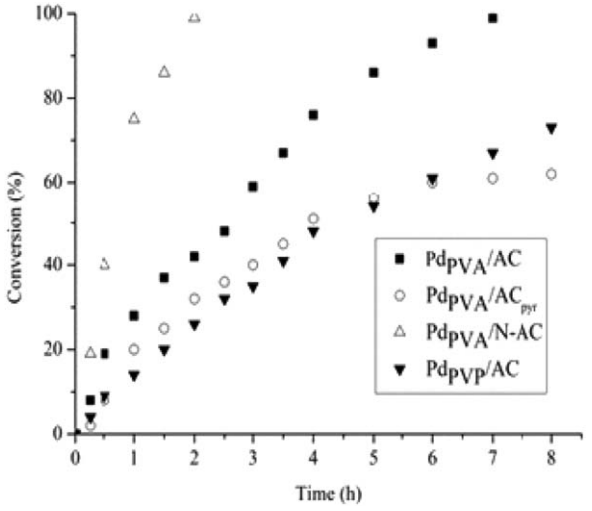

Fig. 15. Reaction profile of Pd catalysts in benzyl alcohol oxidation. Reproduced with permission from ref. [24]. Copyright © 2015 Wiley-VCH.

The introduction of N groups was selectively carried out in the AC structure, through a similar procedure to that of CNT, by adsorbing pyridine on the metal NP surface by using Pd NPs preformed in the presence of a capping agent containing N (polyvinylpyrrolidone (PVP)). As controls, pristine AC and Pd preformed NPs with a non-N-containing capping agent (PVA) were used.

In all cases, good metal dispersion was obtained, but huge differences in catalytic behavior were revealed. Figure 15 reports the reaction profiles of the catalysts in benzyl alcohol oxidation.

When Pd NPs are supported on N-doped carbon, their activity is strongly enhanced with respect to all other catalysts. As the N-content in the samples and the overall basic properties were similar, an obvious conclusion was that the location

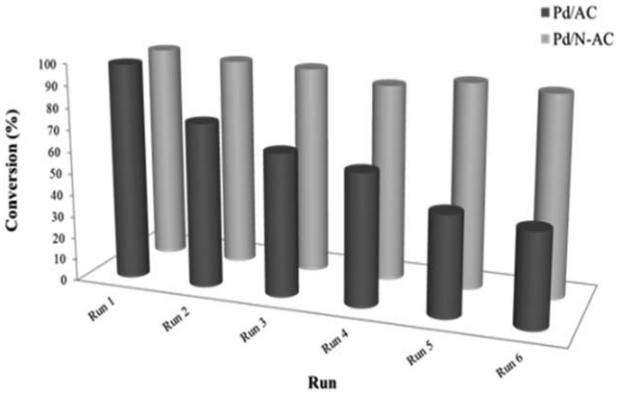

Fig. 16. Stability tests with Pd_{PVA}/AC and Pd_{PVA}/N-AC. Reproduced with permission from ref. [20]. Copyright © 2015 Wiley-VCH.

of the N-groups within the carbon structure was fundamental for improving the activity. This improvement could also be correlated to the enhanced stability of the Pd/N-AC catalyst showed during recycling tests compared with Pd on the bare support (AC; Figure 16).

However, it should be noted that XPS studies showed relevant differences in the nature of the N groups present on different catalysts, the effect of which on the catalytic activity deserve further investigation for clarification.

4. Summary and Outlook

The introduction of N groups within carbon materials was studied to improve and tune the carbon properties as catalytic supports. Studies carried out in our group focused on two different approaches dealing with a post-synthesis modification or the use of N-containing precursors for direct synthesis. In both cases, different types of N-containing groups were introduced (pyridine, pyrrole, or pyridine groups), which were recognized by means of XPS analyses. The relative amount of N groups changed as a function of precursor and temperature treatment during the deposition of metallic NPs, which revealed different abilities of N groups to coordinate to metallic particles. A general trend is that, by increasing the N content, metal NPs appear to be more disperse and stable; thus enhancing the catalytic activity. The position of N groups was shown to be crucial in determining the nature and accessibility of the active site. Inside the pores of CTF, in fact, stable PdH_x particles can be formed; this drastically affects the selectivity of the oxidative reaction. From studies on different modifications of AC, it was also possible to determine that it was not merely the presence of N groups, but also their position that determined an enhancement of the activity of the catalyst. It was indeed shown that the modification should involve the carbon structure to be stable and effective. However, some experiments involving modification of the CNT surface clearly revealed the importance of the nature of the N groups themselves. Further investigations should then be carried out possibly controlling not only the position, but also the N groups introduced.

[1] a) L. Prati, A. Villa, A. R. Lupini, G. M. Veith, *Phys. Chem. Chem. Phys.* **2012**, *14*, 2969–2978; b) S.-Y. Ding, W. Wang, *Chem. Soc. Rev.* **2013**, *42*, 548; c) X. Feng, X. Ding, D. Jiang, *Chem. Soc. Rev.* **2012**, *41*, 6010–6022; d) Y. Zhang, J. Y. Ying, *ACS Catal.* **2015**, *5*, 2681−2691; e) W. J. Lee, U. N. Maiti, J. M. Lee, J. Lim, T. H. Han, S. O. Kim, *Chem. Commun.* **2014**, *50*, 6818; f) P. Zhang, H. Zhu, S. Dai, *ChemCatChem* **2015**, *7*, 2788–2805; g) A. Villa, M. Schiavoni, L. Prati, *Catal. Sci. Technol.* **2012**, *2*, 673–682.

[2] a) R. T. Mayes, P. F. Fulvio, Z. Ma, S. Dai, *Phys. Chem. Chem. Phys.* **2011**, *13*, 2492–2494; b) A. Villa, M. Schiavoni, C. E. Chan-Thaw, P. F. Fulvio, R. T. Mayes, S. Dai, K. L. More, G. M. Veith, L. Prati, *ChemSusChem* **2015**, *8*, 2520–2528.

[3] a) P. Kuhn, M. Antonietti, A. Thomas, *Angew. Chem. Int. Ed.* **2008**, *47*, 3450–3453; b) P. Kuhn, A. Forget, D. S. Su, A. Thomas, M. Antonietti, *J. Am. Chem. Soc.* **2008**, *130*, 13333–13337.

[4] K. Sakaushi, G. Nickerl, H.C. Kandpal, L. Cano-Cortés, T. Gemming, J. Eckert, S. Kaskel, J. van den Brink, *J. Phys. Chem. Lett.* **2013**, *4*, 2977–2981.

[5] K. Sakaushi, G. Nickerl, F.M. Wisser, D. Nishio-Hamane, E. Hosono, H. Zhou, S. Kaskel, J. Eckert, *Angew. Chem. Int. Ed.* **2012**, *51*, 7850–7854.

[6] a) Y. Ham, K. Maeda, D. Cha, K. Takanabe, K. Domen, *Chem. Asian J.* **2013**, *8*, 218–224: b) F. Niu, L. Tao, Y. Deng, H. Gao, J. Liu, W. Song, *New J. Chem.* **2014**, *38*, 5695–5699.

[7] R. Palkovits, M. Antonietti, P. Kuhn, A. Thomas, F. Schüth, *Angew. Chem. Int. Ed.* **2009**, *48*, 6909–6912.

[8] K. Jiang, A. Eitan, L. S. Schadler, P. M. Ajayan, R. W. Siegel, *Nano Lett.* **2003**, *3*, 275–277.

[9] C. E. Chan-Thaw, A. Villa, P. Katekomol, D. Su, A. Thomas, L. Prati, *Nano Lett.* **2010**, *10*, 537–541.

[10] N. Dimitratos, J. A. Lopez-Sanchez, D. Lennon, F. Porta, L. Prati, A. Villa, *Catal. Lett.* **2006**, 147–153.

[11] T. He, L. Liu, G. Wu, P. Chen, *J. Mater. Chem. A* **2015**, *3*, 16235–16241.

[12] a) C.E. Chan-Thaw, A. Villa, L. Prati, A. Thomas, *Chem. Eur. J.* **2011**, *17*, 1052–1057; b) C. E. Chan-Thaw, A. Villa, G. M. Veith, K. Kailasam, L. A. Adamczyk, R. R. Unocic, L. Prati, A. Thomas, *Chem. Asian J.* **2012**, *7*, 387–393.

[13] C. E. Chan-Thaw, A. Villa, D. Wang, V. Dal Santo, A. Orbelli Biroli, G. M. Veith, A. Thomas, L. Prati, *ChemCatChem* **2015**, *7*, 2149–2154.

[14] W. Wunderlich, M. Tanemura in *Advances in Solid State Physics*, *Vol.* 43 (Ed.: B. Kramer), Springer, Berlin, **2003**, pp. 171–180.

[15] a) J. Saha, A. Dandapat, G. De, *J. Mater. Chem.* **2011**, *21*, 11482–11485; b) M. Khanuja, B.R. Mehta, P. Agar, P.K. Kulriya, D.K. Avasthi, *J. Appl. Phys.* **2009**, *106*, 093515–093522.

[16] T. Yokosawa, T. Alan, G. Pandraud, B. Dam, H. Zandbergen, *Ultramicroscopy* **2012**, *112*, 47–52.

[17] a) W. C. Ketchie, Y. Fang, M. S. Wong, M. Murayama, R. J. Davis, *J. Catal.* **2007**, *250*, 94–101; b) L. Prati, P. Spontoni, A. Gaiassi, *Top. Catal.* **2009**, *52*, 288–296; c) D. Wang, A. Villa, D. Su, L. Prati, R. Schloegl, *ChemCatChem* **2013**, *5*, 2717–2723.

[18] a) A. Hirsch, *Angew. Chem. Int. Ed.* **2002**, *41*, 1853–1859; b) Y. P. Sun, K. Fu, Y. Lin, W. Huang, *Acc. Chem. Res.* **2002**, *35*, 1096–1104; c) P. Serp, M. Corrias, P. Kalck, *Appl. Catal. A* **2003**, *253*, 337–358; d) D. S. Su, S. Perathoner, G. Centi, *Chem. Rev.* **2013**, *113*, 5782−5816; e) D-W. Wang, D. S. Su, *Energy Environ. Sci.* **2014**, *7*, 576–591.

[19] a) Y.Q. Wang, F.Q. Zhang, P.M.A. Sherwood, *Chem. Mater.* **1999**, *11*, 2573–2583; b) J. Li, M. J. Vergne, E. D. Mowles, W. H. Zhong, D. M. Hercules, C. M. Lukehart, *Carbon* **2005**, *43*, 2883–2893; c) A. Rasheed, J. Y. Howe, M. D. Dadmun, P. F. Britt, *Carbon* **2007**, *45*, 1072–1080; d) A. B. Dongil, B. Bachiller-Baeza, A. Guerrero-Ruiz, I. Rodríguez-Ramos, A.

Martínez-Alonso, J. M. D. Tascón, *J. Colloid Interface Sci.* **2011**, *355*, 179–189.
[20] a) C. P. Ewels, M. Glerup, *J. Nanosci. Nanotechnol.* **2005**, *5*, 1345–63; b) S. Kundu, W. Xia, W. Busser, M. Becker, D. A. Schmidt, M. Havenith, M. Muhler, *Phys. Chem. Chem. Phys.* **2010**, *12*, 4351–4359.
[21] L. Prati, A. Villa, C. E. Chan-Thaw, R. Arrigo, D. Wang, D. S. Su, *Faraday Discuss.* **2011**, *152*, 353–365.
[22] R. Arrigo, M. Haevecker, S. Wrabetz, R. Blume, M. Lerch, J. McGregor, E. P. J. Parrott, J. A. Zeitler, L. F. Gladden, A. Knop-Gericke, R. Schloegl, D. Su, *J. Am. Chem. Soc.* **2010**, *132*, 9616.
[23] A. Villa, D. Wang, P. Spontoni, R. Arrigo, D. Su, L. Prati, *Catalysis Today* **2010**, *157*, 89–93.
[24] C. E. Chan-Thaw, A. Villa, G. M. Veith, L. Prati, *ChemCatChem* **2015**, *7*, 1338–1346.

Received: October 20, 2015
Published online: ■■

